

Chirality affects cholesterol-oxysterol association in water, a computational study

Supporting Information

Michał Markiewicz¹, Robert Szczelina², Bożena Milanović¹, Witold K. Subczynski³, Marta Pasenkiewicz-Gierula¹

¹Department of Computational Biophysics and Bioinformatics, Faculty of Biochemistry, Biophysics, and Biotechnology, Jagiellonian University, Krakow, Poland

²Division of Computational Mathematics, Faculty of Mathematics and Computer Science, Jagiellonian University, 30-348 Krakow, Poland

³Department of Biophysics, Medical College of Wisconsin, Milwaukee, Wisconsin 53226, USA

*Corresponding authors:

Michał Markiewicz, e-mail: m.markiewicz@uj.edu.pl;

Marta Pasenkiewicz-Gierula, e-mail: marta.pasenkiewicz-gierula@uj.edu.pl

Materials and Methods

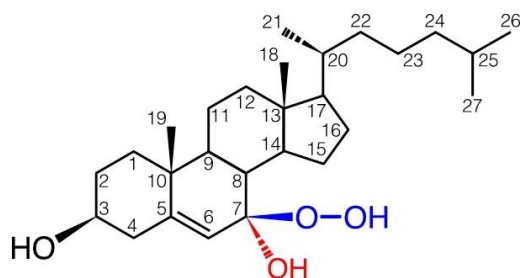


Figure S1. Molecular structure of cholesterol (*black*, Chol), C7-hydroxycholesterol (*black* and *red*, 7-OH-Chol) and C7-hydroperoxycholesterol (*black* and *blue*, 7-OOH-Chol). The C7-OH group of 7 β -OH-Chol is in *red*, and the C7-OOH group of 7 α -OOH-Chol is in *blue* (α and β are chiral forms of the hydroxy and hydroperoxy groups). The Chol atoms are numbered according to the IUPAC convention (1). The chemical symbol for carbon atoms, C, is omitted and the hydrogen atoms are not shown except for the sterol polar groups, where the H atoms are explicitly included.

Umbrella sampling

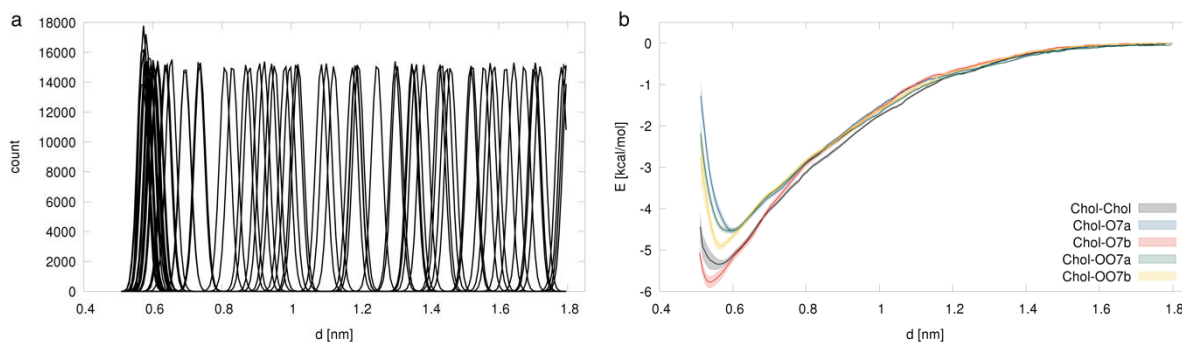


Figure S2. (a) Histograms of umbrella sampling for calculating PMF, bin size = 0.1 nm; (b) 500 bootstrap profiles used to calculate the average free energy profiles as functions of the C13-C13 distance. Error bars were represented as mean square displacements of the bootstrap profiles obtained.

Free energy perturbation

In this free energy calculation, a sterol molecule is transformed from a state A where it interacts with the water molecules to a state B, where this interaction is totally switched off. The latter means that the sterol molecule still occupies a certain space in the water box but has no effect on the water, thus the sterol and the water are decoupled; such a state corresponds to Chol in vacuum. This procedure is called “alchemical transformation” and involves the generation of a number of non-physical intermediate states connecting A to B. Transformation is calculated as a function of a coupling parameter, λ , which varies between 0 and 1 when the system goes from the initial state, A, to the final state, B, and indicates the level of change that has taken place in a given intermediate state.

Voronoi diagram

The Voronoi diagram partitions the Euclidean space with n specified points (objects) called sites, into n Voronoi regions that fit closely to each other. Each site lies in precisely one region called the Voronoi cell of this site (Fig. 3). All points in the Euclidean space enclosed in the Voronoi cell are closer to its site than to any other site. All cells constitute the whole space, and their sides are, in general, polygons called faces. A face consists of all points in the space that are equidistant from precisely two sites. Two sites whose cells share a common face, are called neighbours. The boundary between two objects, e.g. sterol and water or water layers L_n and L_{n+1} , is defined as a set of all common sides of the neighbouring Voronoi cells of both objects (2D illustration is in Fig. 4 of the main text).

The Voronoi diagram was generalized to account for the Periodic Boundary Conditions. In this study it was applied to analyse the geometric properties of objects in the computational systems; for this purpose custom-tailored scripts were written in Python. The DMG- α library (2) [Szczelina (www), 2016] was used to create 3D Voronoi cells around heavy atoms of the molecules (both sterols and solvent). The hydrogen atoms were excluded because it was shown that their inclusion occasionally introduced discrepancies with theoretical and experimental results (e.g. the computed vs. expected volume of the molecules) (2).

Non-linear least squares fitting

The sterol-bound water molecules exchange with bulk water. Here, the characteristic exchange times of three groups of water molecules, i.e., clathrating a sterol molecule, H-bonded to a sterol molecule and belonging to *LI*, are assessed. To evaluate an exchange time, at a certain instant (initial time) the number of water molecules belonging to a group is counted (initial set) and then the number of the water molecules that remained from the initial set, is counted every 400 fs. For each group, the number decreases due to the exchange and after 50 ps the set contains none of the water molecules that had initially been present, so the counting is then stopped. Water molecules which “returned” to the current set were not considered. The time profile of the decreasing number of water molecules is an exponential decay curve. To smooth the curve and get rid of the effect of the choice of the initial time, the counting procedure is repeated every 25 ps of the 5-ns trajectory. This generates 200 individual decay curves for each group and each curve consists of 126 points. The individual curves are summed up, averaged and normalised to an initial value of 1.0. The curves are fitted with the sum of two exponential functions to obtain the characteristic exchange time (τ_1), *i.e.* the time after which the number of the initially bound water molecules decreases to $1/e \approx 0.37$ and the contribution (A_i , pre-exponential factor) of each component in the total decay. To determine the four unknown parameters of each decay curve (obtained from averaging of 200 individual curves) the nonlinear least-squares minimisation Trust Region Reflective (4) method was used. The decay curve was fitted with a two-exponential function (1)

$$F(t; \tau_1, \tau_2, A_1, A_2) = \sum_1^2 A_l \exp\left(-\frac{t}{\tau_l}\right) \quad (1)$$

where A_1 and A_2 are > 0 and ≤ 1.0 and $\tau_1 > 0$.

To assess the goodness of fit, a reduced χ^2 was calculate according to formula (2)

$$\chi^2 = \sum_1^N \frac{(D_i - F_i)^2}{(N - 1 - 4)\sigma_i^2} \quad (2)$$

where D_i and F_i are the i -th value of the decay curve and the fitted function, respectively, σ_i is the standard deviation of each $N = 126$ decay curve points, and 4 is the number of fitted parameter.

The reduced χ^2 (χ^2 per degree of freedom) is 1.0 when the fit is perfect.

Results

Sterol-water interaction

Initial hydration

The generation of a plausible initial reaction of water on the appearance of a sterol molecule required the initial state of the system to be properly defined. For this purpose, the algorithm for the initial hydration of the molecule (“hydrating algorithm”) used in GROMACS was carefully inspected. The algorithm uses pre-defined vdW radii of the atoms and places the hydrating water molecules at distances from the hydrated molecule not smaller than the scaled sums of the atomic vdW radii. Here only H, C and O atoms are considered as relevant for the present case. In the “hydrating algorithm” the following values for the atomic vdW radii for these atoms are used: H = 0.12 nm; C = 0.17 nm; O = 0.152 nm and the scaling factor $\lambda = 0.57$, as “0.57 yields density close to 1000 g/l for proteins in water” (3). As a result, the cut-off distances for water molecules are $(0.12 + 0.12) \times 0.57 = 0.1368$ nm for $H_{\text{wat}}-H_{\text{ste}}$; 0.1653 nm for $H_{\text{wat}}-O_{\text{ste}}$; and 0.1938 nm for $O_{\text{wat}}-O_{\text{ste}}$ distances. These distances are significantly smaller than the sigmas (twice the vdW radii) in the vdW term of the OPLSAA potential energy function (0.35 and 0.25 nm for C and H atoms in the hydrocarbon chain, respectively; 0.34 nm for the hydroxyl O atom; 0.315 and 0 nm for the O and H atoms of the TIP3P water, respectively) used here.

Direct application of the “hydrating algorithm” caused a rapid increase in the sterol temperature (Fig. S3a), dumped with the 0.01 ps time constant, and the sinusoidal behaviour of the *LI* water-sterol distance (Fig. S3b) during the initial 2 ps of MD simulation. This undesired effect was eliminated when λ was increased to 0.9. For this scaling factor, the density of water is well preserved, of 1000.4 g/l, there is no temperature jump in the system—the sterol and water temperature oscillates around the set value of 310 K (Fig S3c) and *LI* water-sterol distance steadily decreases to a constant value (Fig. S4).

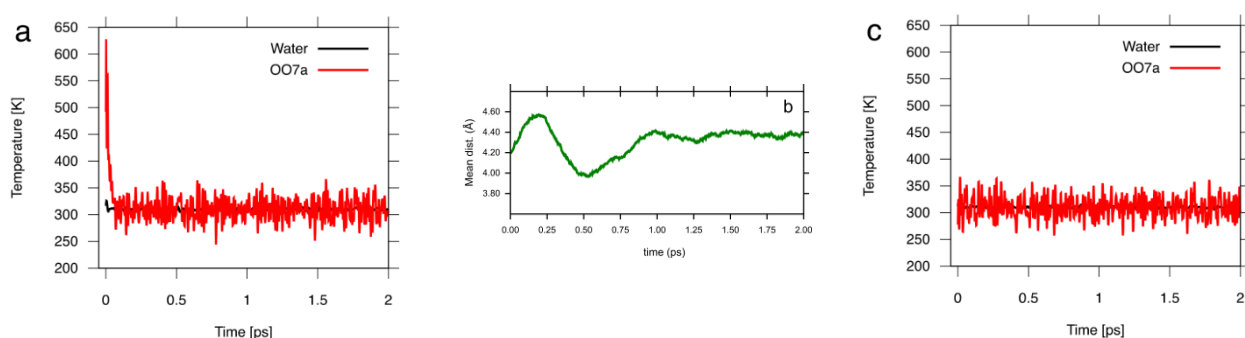


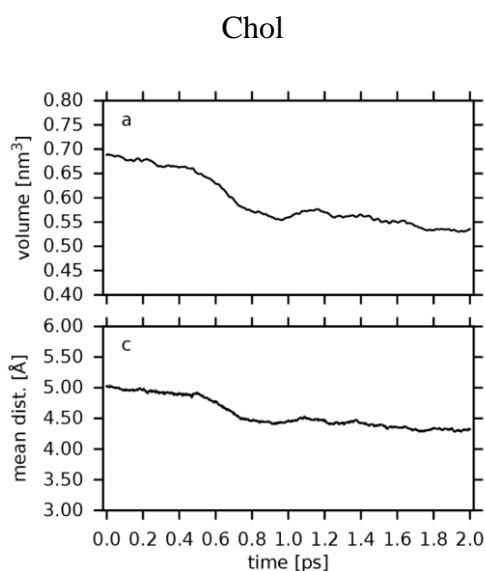
Figure S3. (a) Time profiles of the sterol and water temperature for scaling factor $\lambda = 0.6$; (b) time profile of the *LI* water-sterol distance for $\lambda = 0.6$; and (c) time profiles of the sterol and water temperature for scaling factor $\lambda = 0.9$; water temperature – black line, sterol temperature – red line.

Short-term effects

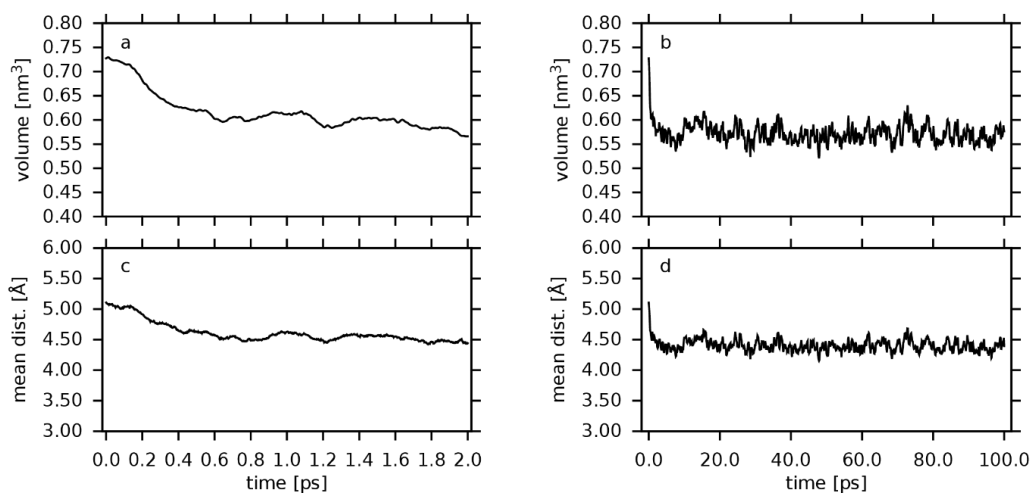
The ‘short-term’ is here a 2-ps period which starts at the moment of a sterol monomer appearance (0 fs) in the water box; it corresponds to the first 2-ps fragment, recorded every 2 fs, of MD simulation. The system consisting of the sterol molecule and water was not optimised before starting MD simulation but the sterol molecule and the water box into which the molecule was inserted were previously pre-equilibrated in separate MD simulations (sterol was MD simulated in water). When hydrating the pre-equilibrated sterol molecule the described above the scaling factor $\lambda=0.9$ was used (cf. sec. above).

The short-term ‘reaction’ of water molecules on the sterol presence was assessed by determining the time dependence of (1) the average distance between the sterol molecule and the water molecules from the first hydration shell (LI) as well as the average volume available to the sterol molecule (Fig. S4), obtained from the Voronoi diagram analysis; (2) the electrostatic and vdW energies of sterol-water and water-water interactions (Fig. S5), obtained directly from unrestricted MD simulations.

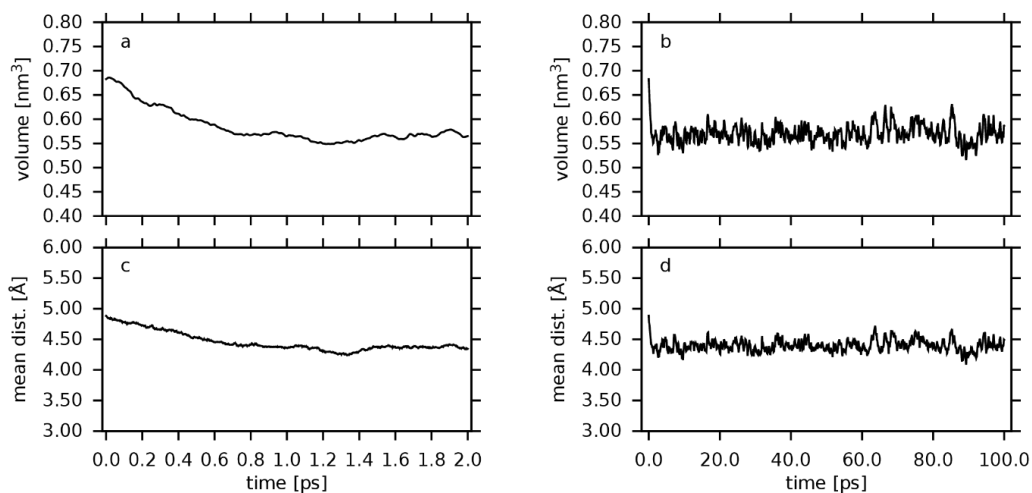
Time profiles of the mean volume available to the sterol molecule and the mean distance between oxChol and the water molecules from LI during the first 2 ps and the first 100 ps of MD simulation



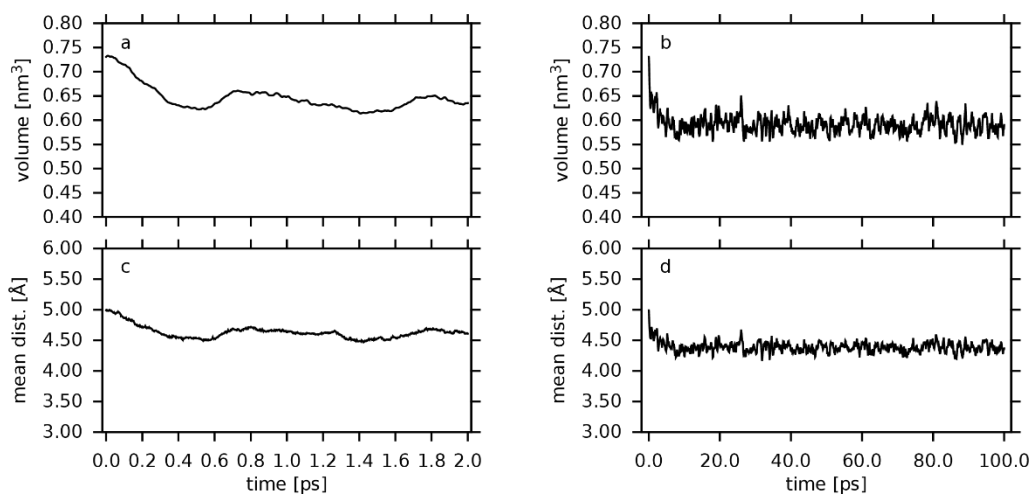
7 α -OH-Chol



7 β -OH-Chol



7 α -OOH-Chol



7 β -OOH-Chol

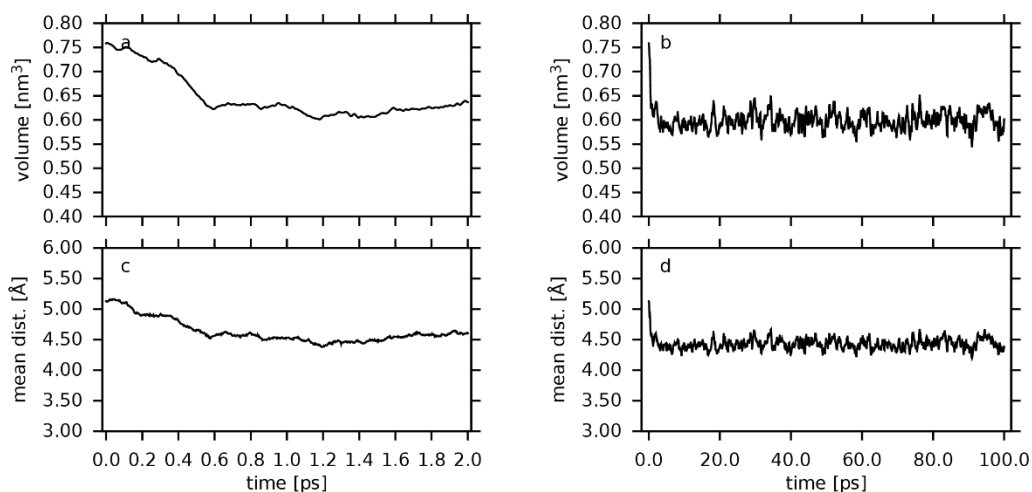
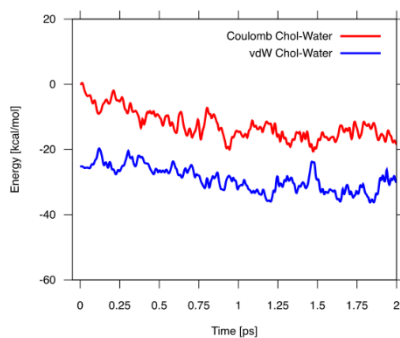


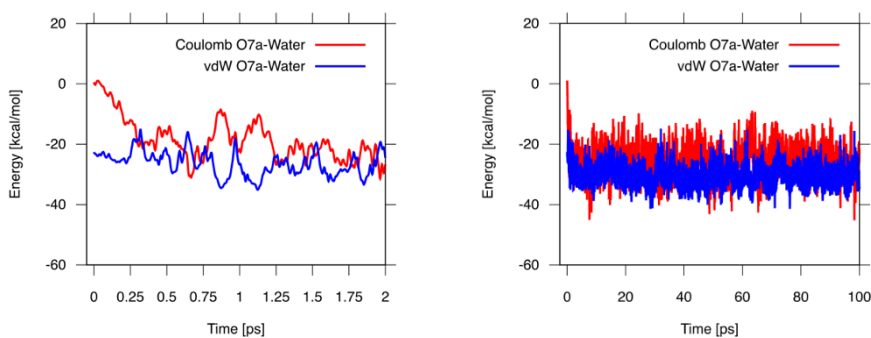
Figure S4. Mean (a, b) volume available to the sterol molecule and (c, d) distance between oxChol and the water molecules from *L1* as a function of time, during (a, c) 2 ps plotted every 2 fs, (b, d) 100 ps, plotted every 100 fs. Abbreviations used in the panel titles are explained in Fig. S1.

Time profiles of the sterol-water Coulomb (electrostatic) and vdW energies during the first 2 ps and the first 100 ps of MD simulation

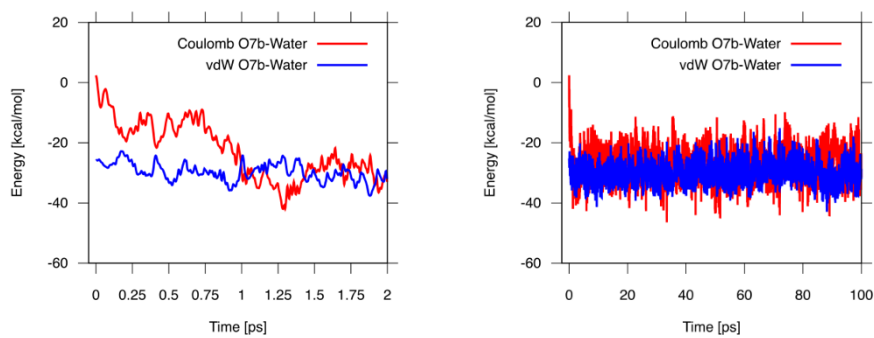
Chol



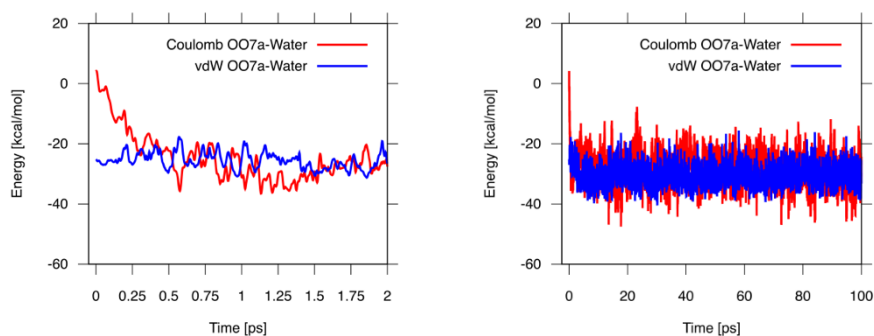
7 α -OH-Chol



7 β -OH-Chol



7α -OOH-Chol



7β -OOH-Chol

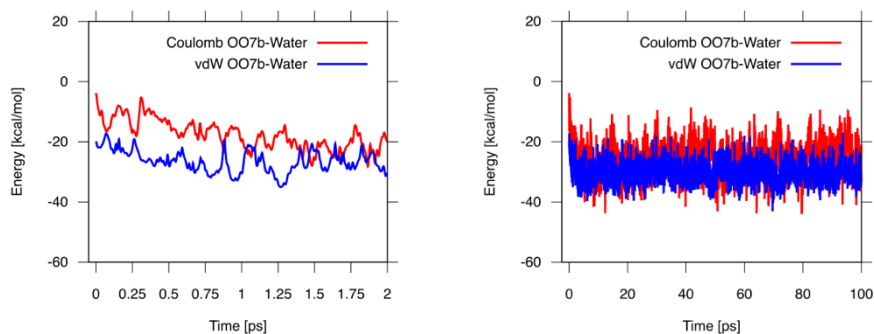
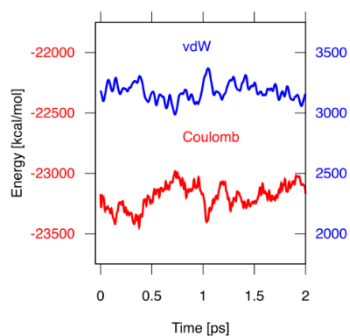


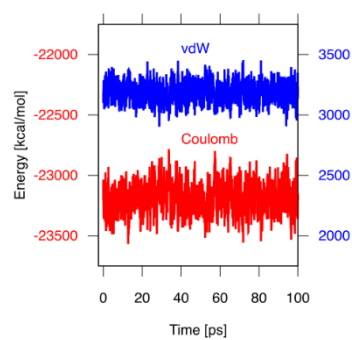
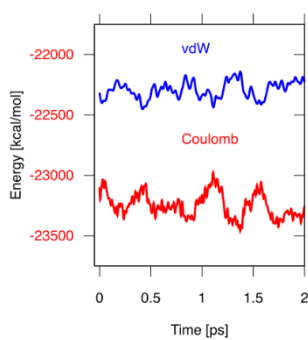
Figure S5. Interaction energies of the pre-equilibrated sterol with water (sterol-water interaction), electrostatic (*red*); vdW (*blue*), during (LEFT) 2 ps, (RIGHT) 100 ps, plotted every 2 fs. Abbreviations used in the panel titles are explained in Fig. S1.

Time profiles of the water-water Coulomb (electrostatic) and vdW energies during the first 2 ps and the first 100 ps of MD simulation of an sterol monomer in water

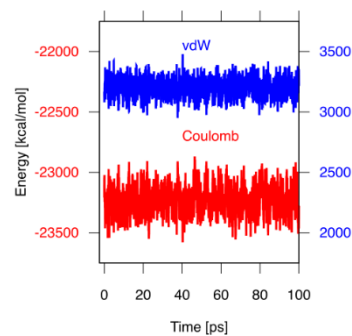
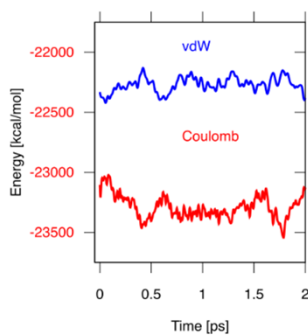
Chol



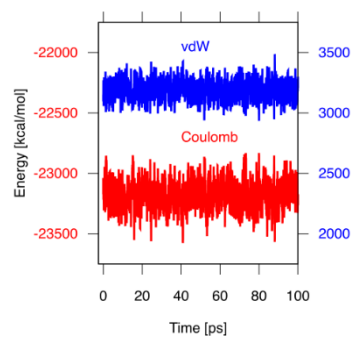
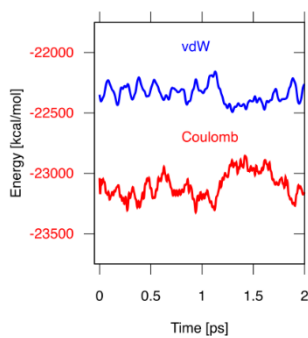
7 α -OH-Chol



7 β -OH-Chol



7 α -OOH-Chol



7 β -OOH-Chol

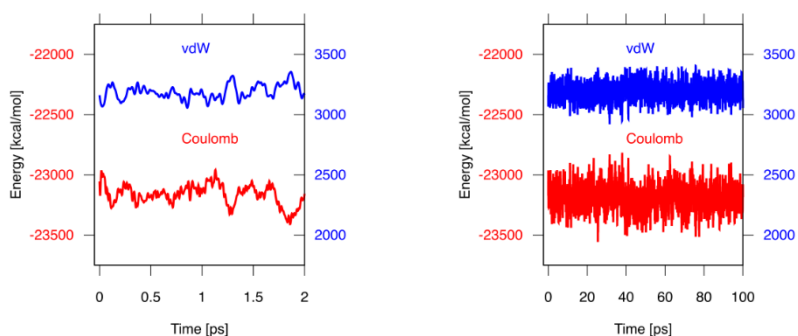


Figure S6. Energies of water-water interactions in the presence of a sterol monomer, electrostatic (*red*), vdW (*blue*), during (LEFT) 2 ps, (RIGHT) 100 ps, plotted every 2 fs. Abbreviations used in the panel titles are explained in Fig. S1.

Sterol-water interactions at equilibrium

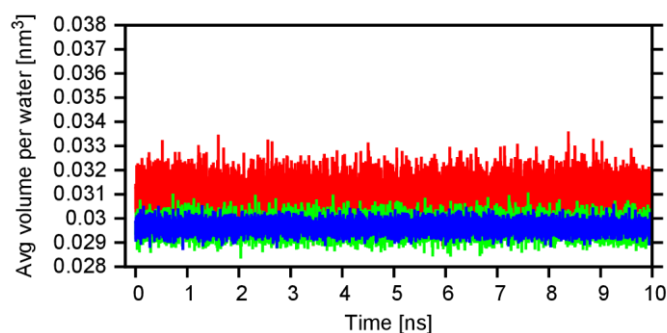


Figure S7. Average volume of a water molecule in the first (*L1*, *red*), second (*L2*, *green*) and third (*L3*, *blue*) hydration shells.

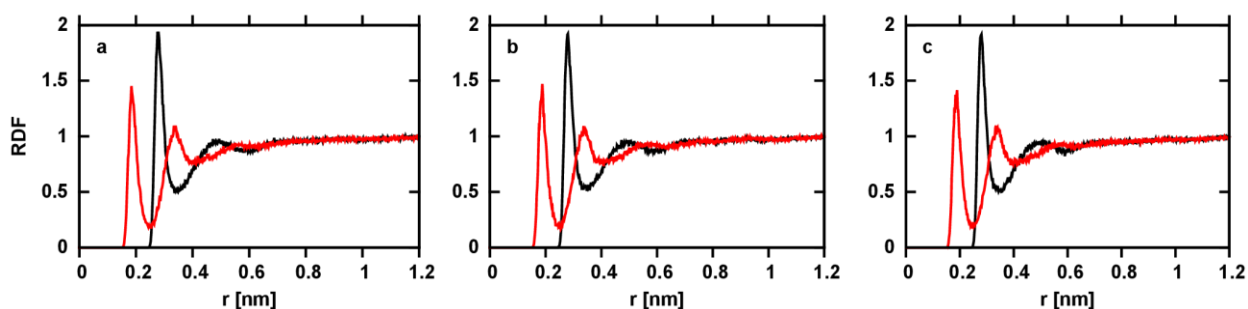


Figure S8. Radial distribution functions (RDF) of water oxygen atoms relative to the sterol C3-OH group of (a) Chol; (b) 7-OH-Chol; (c) 7-OOH-Chol. C3-OH O atom (*black*), C3-OH H atom (*red*).

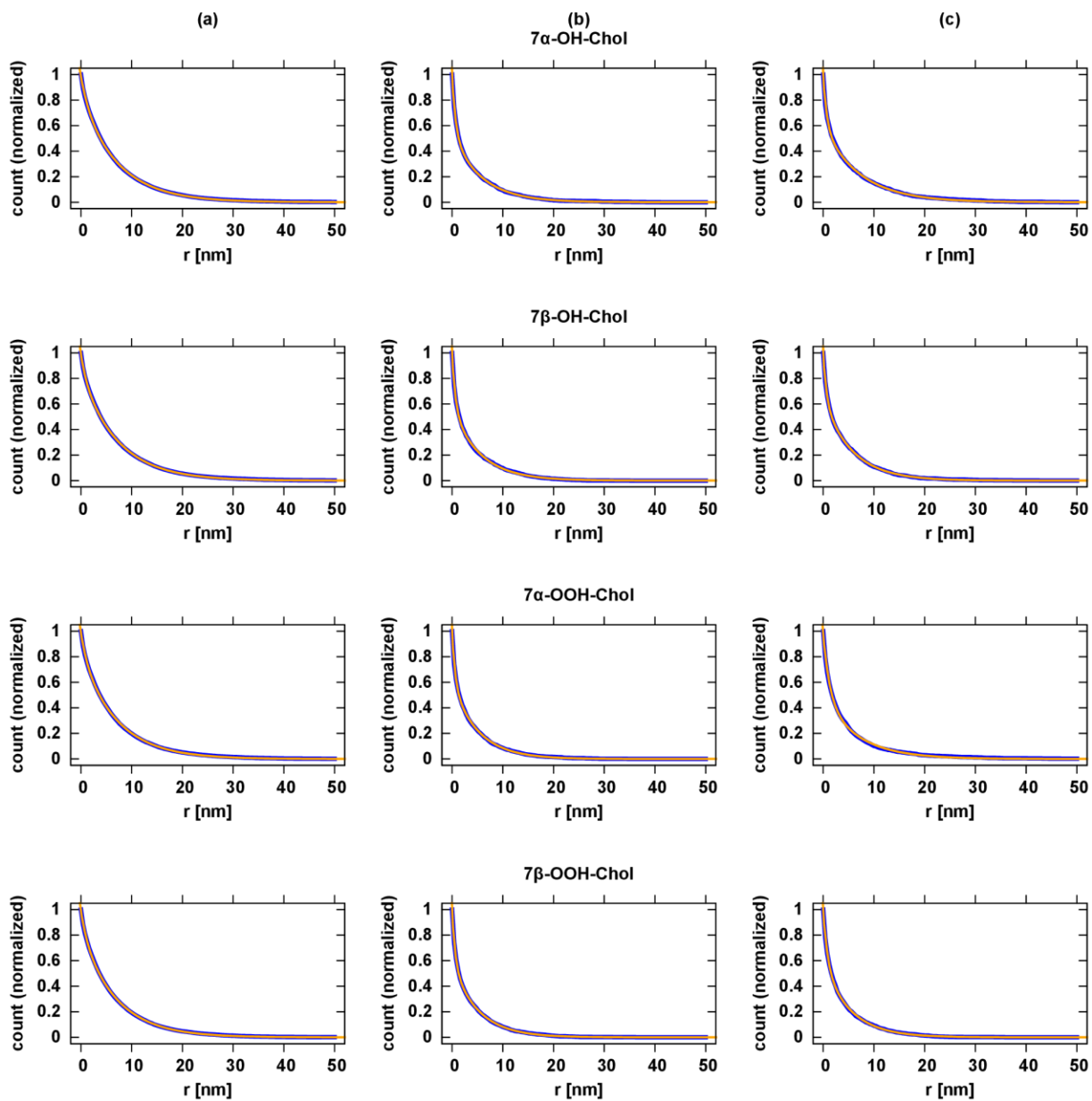
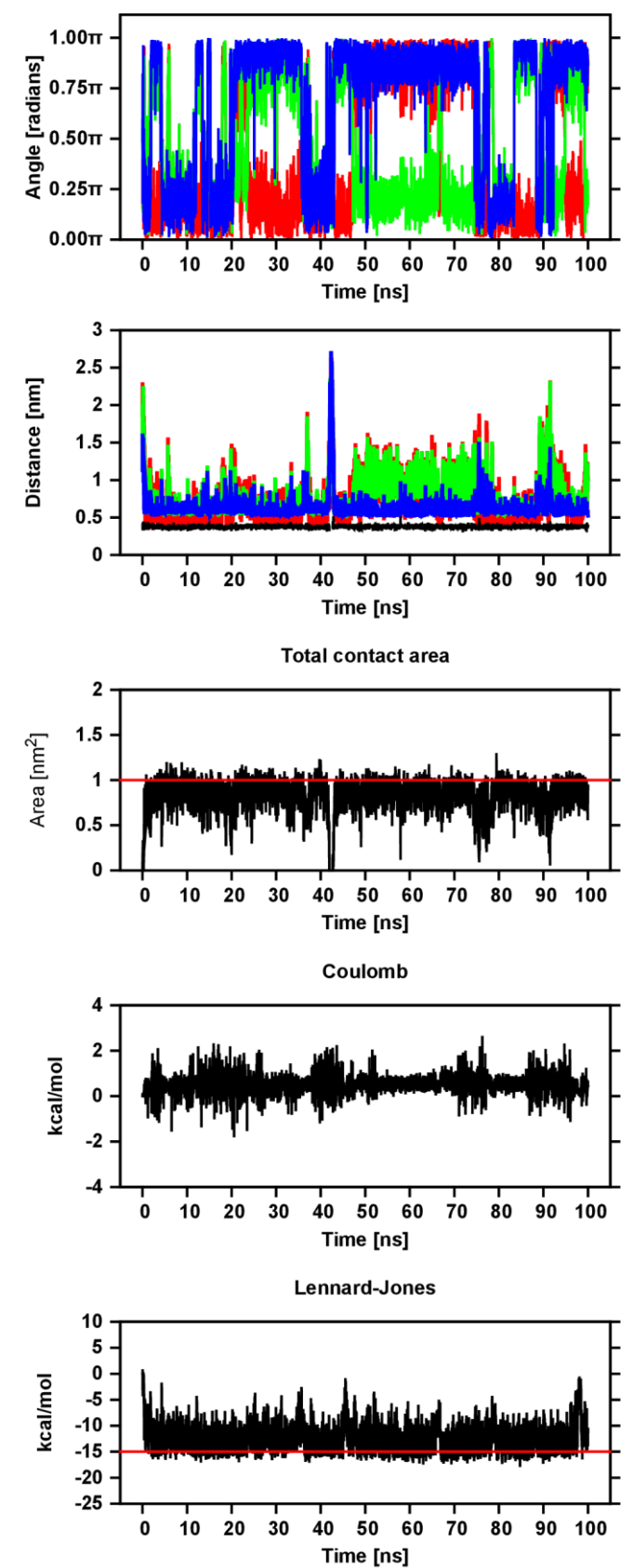


Figure S9. Exchange of the oxChol-bound water with bulk. (a) clathrating, (b) H-bonded to C3-OH, and (c) H-bonded to C7-OH or C7-OOH. The decay curve (blue) of the initial number of water molecules is fitted to the two exponential functions (orange); the blue and orange curves are superimposed. The reduced χ^2 of all fits is essentially 1.0, which indicates perfect fits.

Sterol-sterol aggregation in water

Chol-Chol (100-ns)



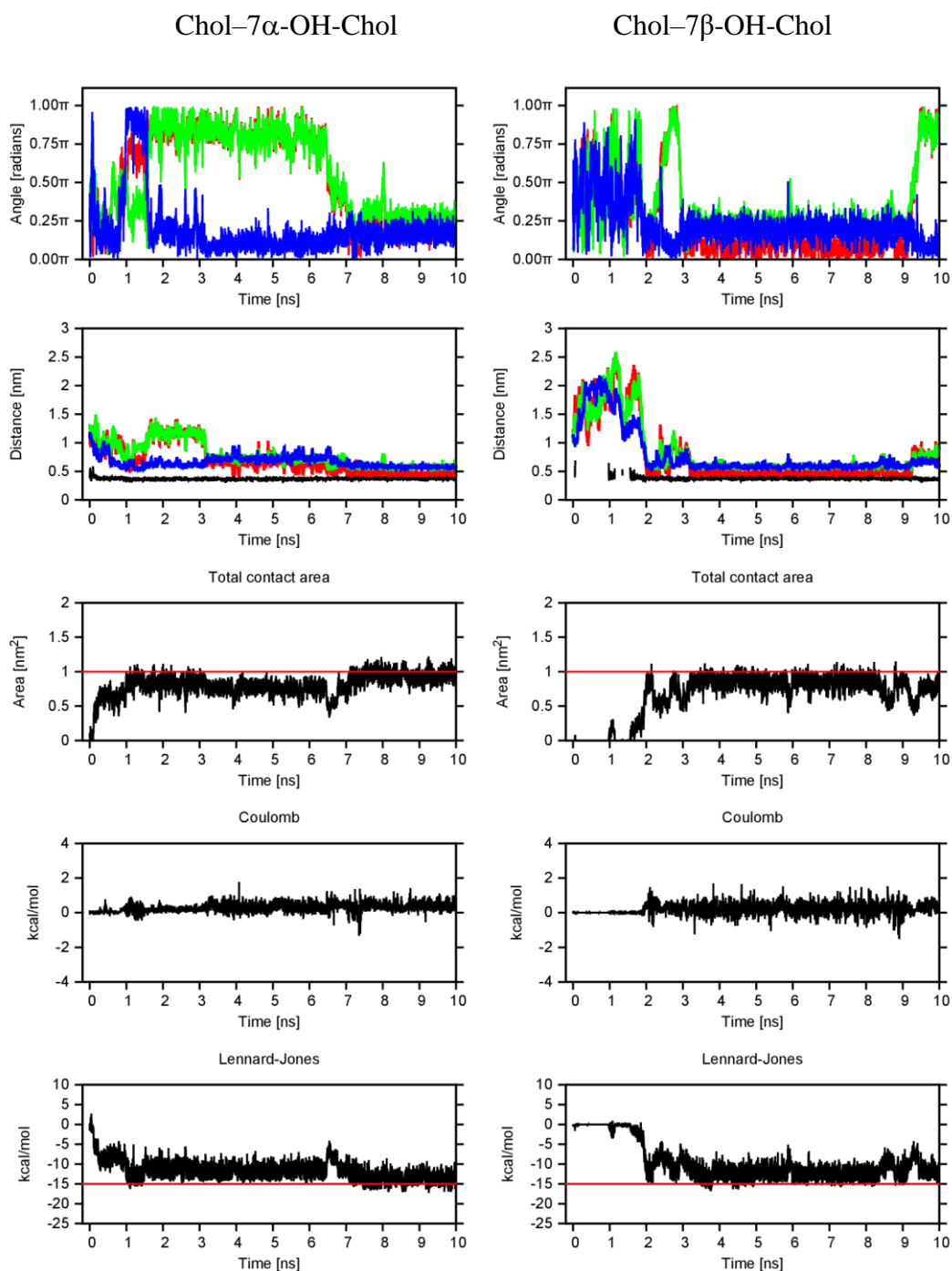


Figure S10. Time courses of the relative orientation, distance, contact area and intermolecular interaction energies of Chol and (TOP) Chol (100-ns MD simulation); (LEFT) 7 α -OH-Chol and (RIGHT) 7 β -OH-Chol in water before and after dimer formation. From top to bottom: angles between corresponding vectors, \mathbf{u} (red), \mathbf{v} (green) and \mathbf{w} (blue); distances between the C6 (red), C10 (green) and C13 (blue) atoms (cf. sec. 2.4.2) and the smallest distance between any atoms (black), of both molecules; area of the contact surface; energies of Coulomb (blue); and vdW (green). Noisy fragments of the time profiles indicate the dynamic nature of the relatively stable dimer, whereas temporary simultaneous changes of 180° (π) in any two angles illustrate that one

molecule reverses its orientation relative to the other. The horizontal *red* lines are drawn to help compare the values of quantities in the plots.

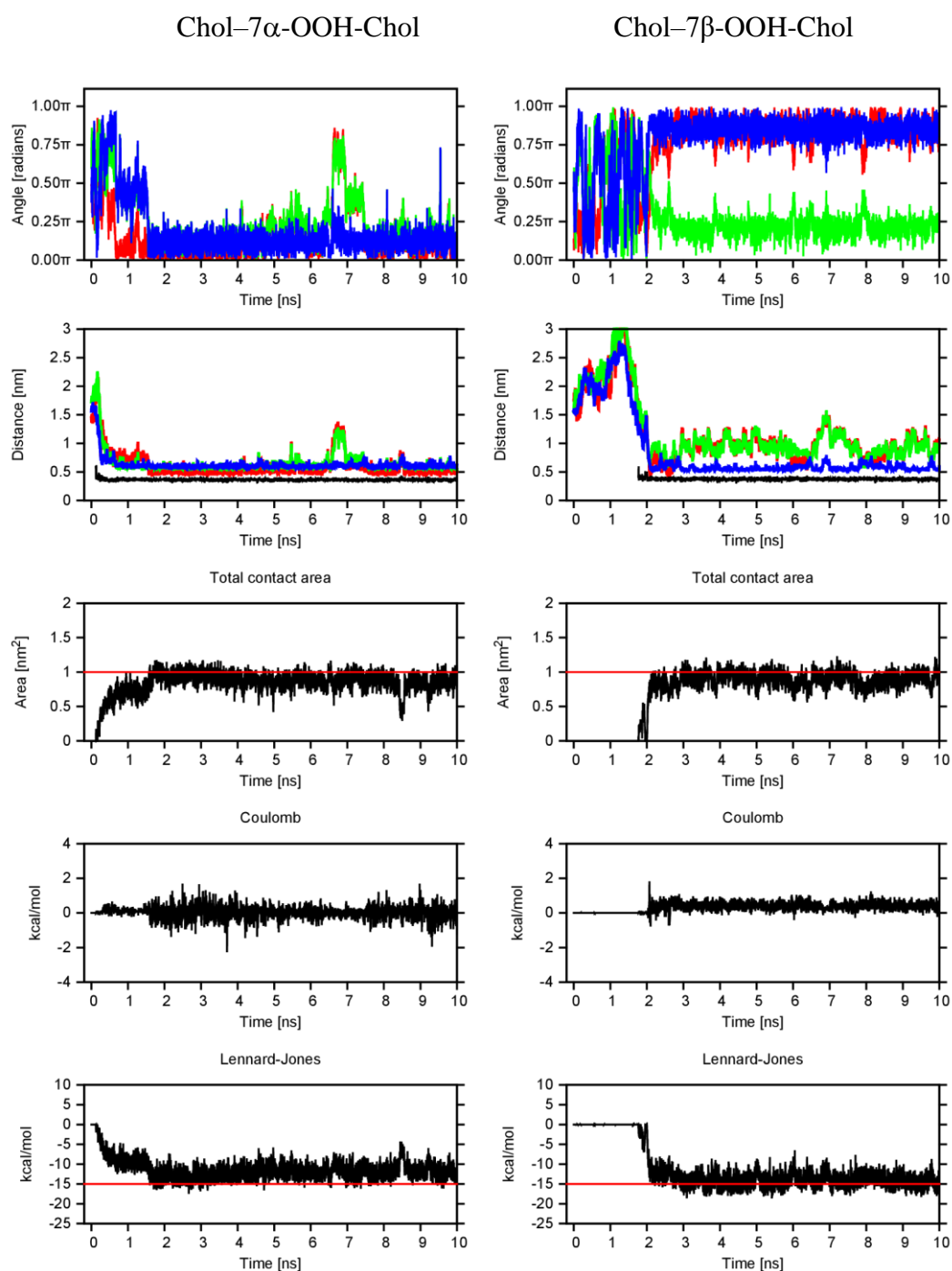
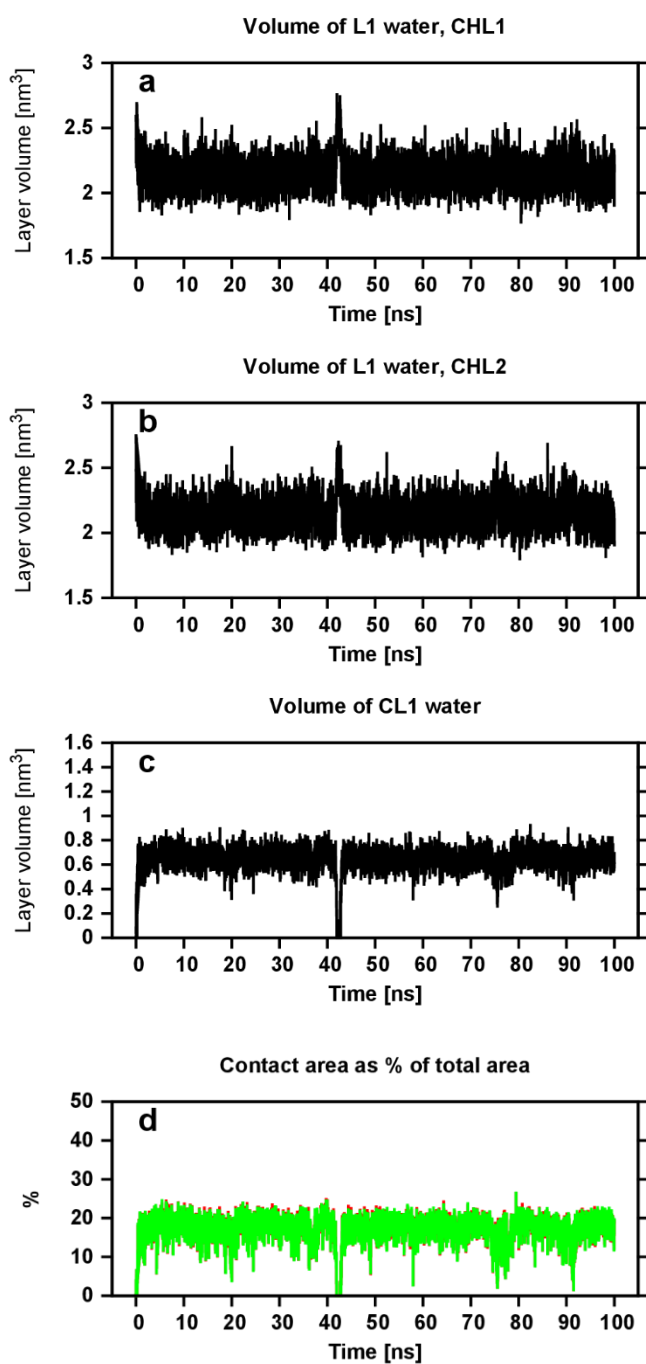


Figure S11. Time courses of the relative orientation, distance, contact area and intermolecular interaction energies of Chol and (LEFT) 7 α -OOH-Chol and (RIGHT) 7 β -OOH-Chol in water before and after dimer formation. From top row to bottom: angles between corresponding vectors, *u* (red), *v* (green) and *w* (blue); distances between the C6 (red), C10 (green) and C13 (blue) atoms (cf. sec. 2.4.2) and the smallest distance between any atoms (black), of both molecules; area of the

contact surface; Coulomb and vdW energies. Noise around the time profiles indicate the dynamic nature of the relatively stable dimer, whereas temporary simultaneous changes of 180° (π) in any two angles illustrate that one molecule reverses its orientation relative to the other. The horizontal *red* lines are drawn to help compare the values of quantities in the plots.

Dehydration of the contacting surfaces of the aggregating sterols

Chol-Chol (100 ns)



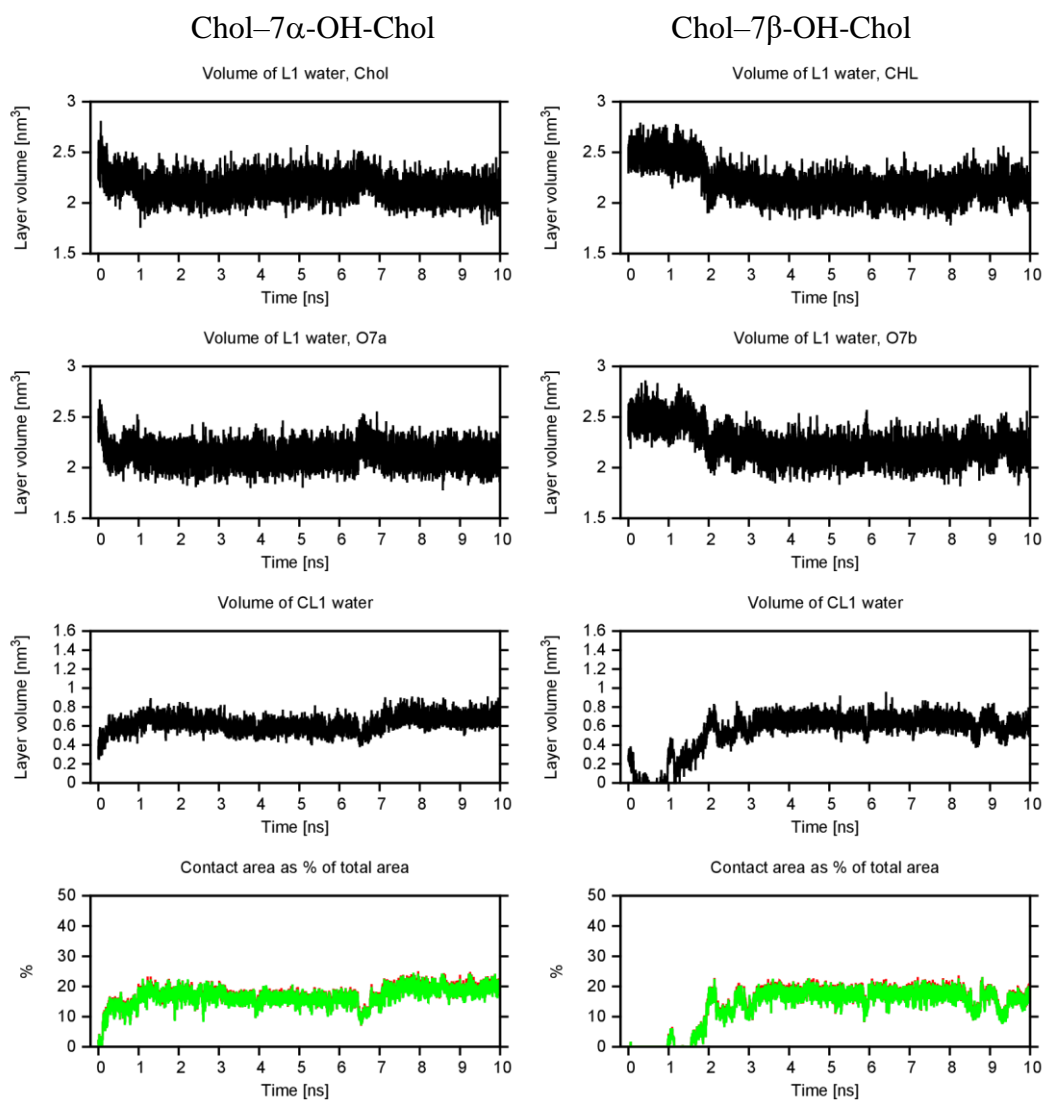


Figure S12. Time profiles of the volume of the hydration layers and the area of the contact surface of Chol and (TOP) Chol (100-ns MD simulation); (LEFT) 7 α -OH-Chol (O7a) and (RIGHT) 7 β -OH-Chol (O7b) in water before and after dimer formation. From top row to bottom: *L1* water of Chol; *L1* water of Chol or oxChol; cross-layer *CL1* water of both molecules and area of the contact surface as % of the total area of each sterol molecule – the *red* (Chol) and *green* (Chol2 or oxChol) lines overlap.

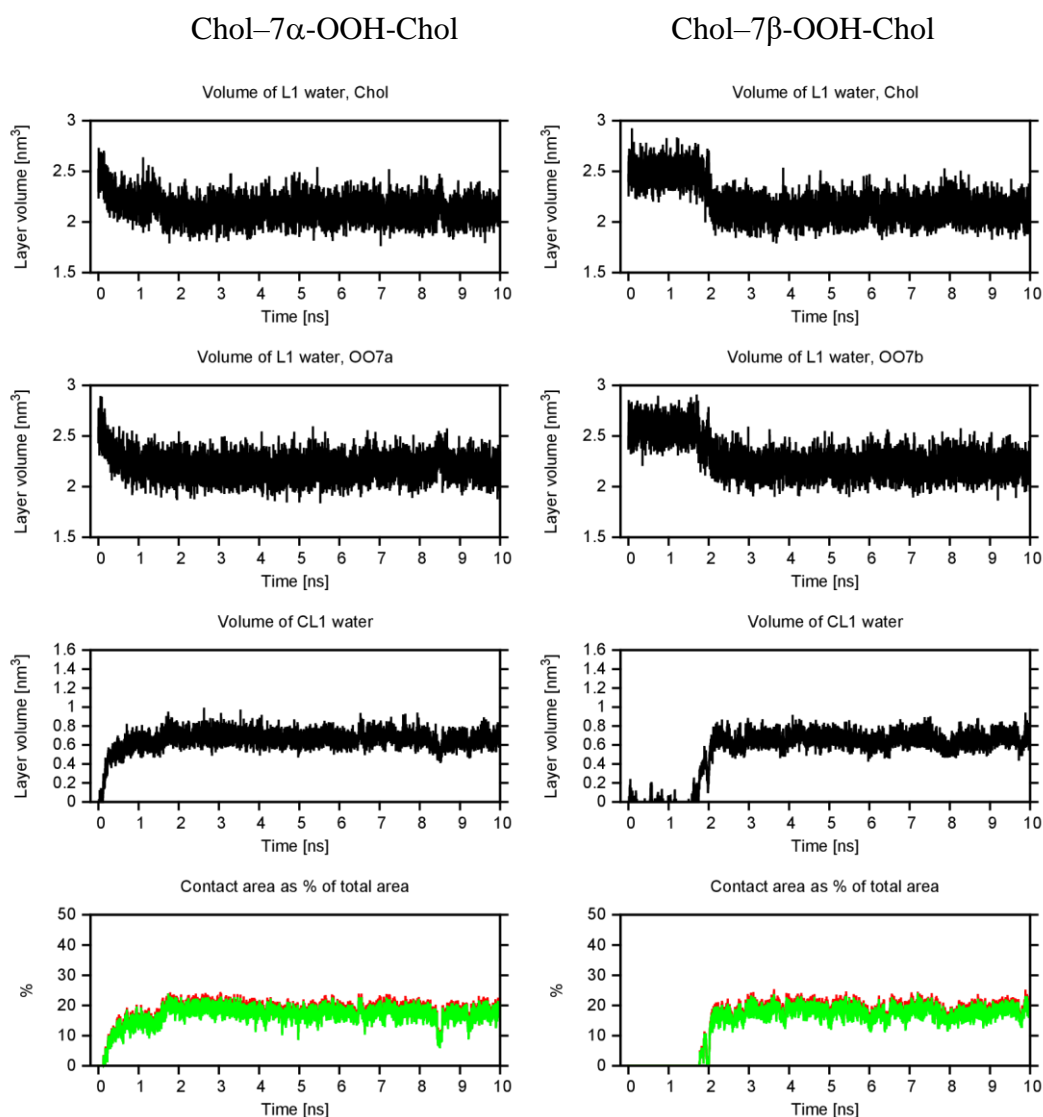


Figure S13. Time profiles of the volume of the hydration layers and the area of the contact surface of Chol and (LEFT) 7 α -OOH-Chol (OO7a) and (RIGHT) 7 β -OOH-Chol (OO7b) in water before and after dimer formation. From top row to bottom: *L1* water of Chol; *L1* water of oxChol; cross-layer *CL1* water of both molecules and area of the contact surface as % of the total area of each sterol molecule – the *red* (Chol) and *green* (oxChol) lines overlap.

Relatively stable configurations of the sterol molecules in the dimer

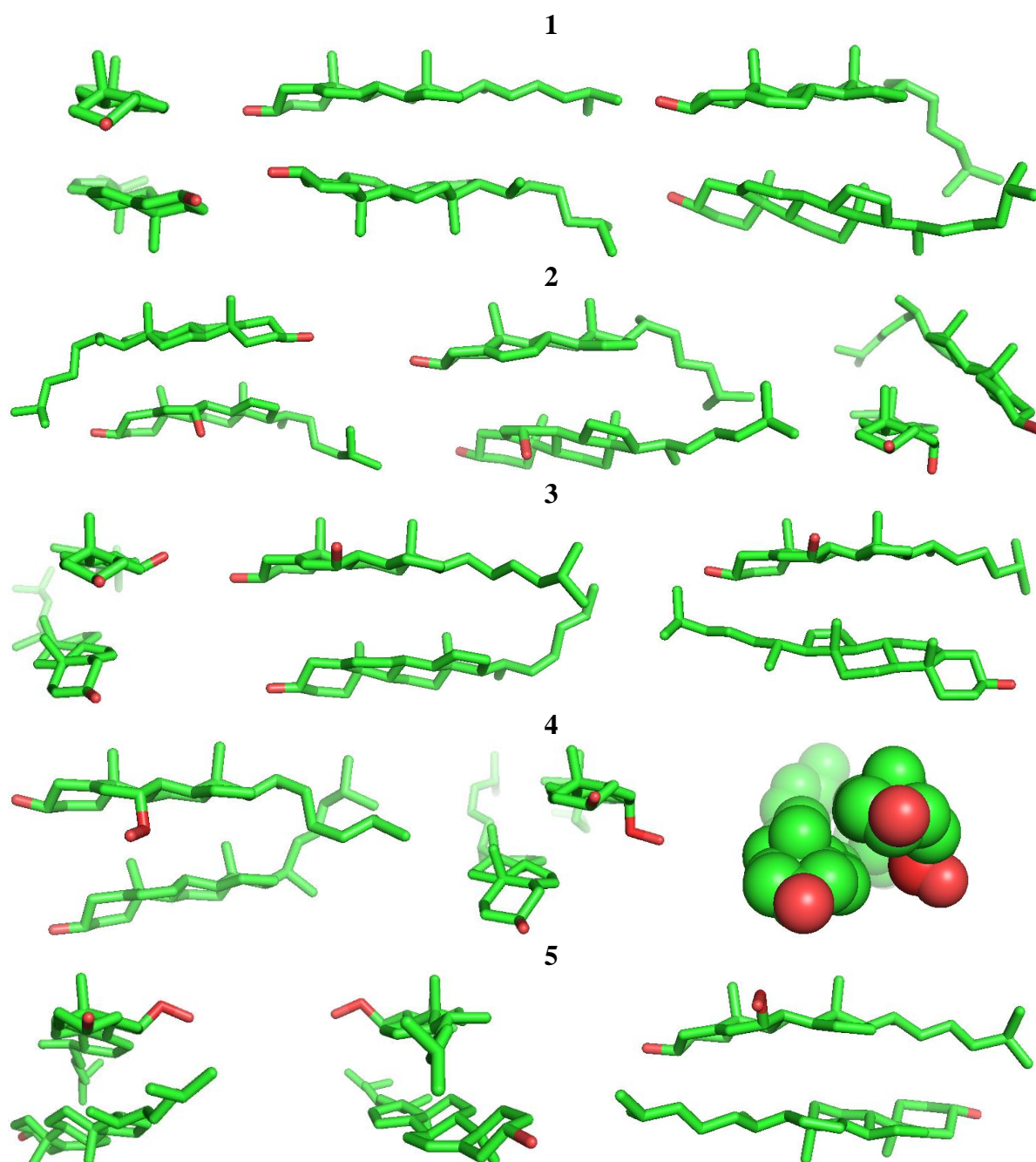


Figure S14. Snapshots of the (Top, row #1) Chol–Chol, (row #2) Chol–7 α -OH-Chol, (row #3) Chol–7 β -OH-Chol, (row #4) Chol–7 α -OOH-Chol, (Bottom, row #5) Chol–7 β -OOH-Chol; dimers. Top, row #1: smooth-smooth, head-to-head front (LEFT) and side (middle) view at 3 ns, smooth-rough, head-to-head (RIGHT) at 9 ns, of MD simulation; row #2: smooth-rough, head-to-tail (LEFT) at 4 ns, smooth-rough, head-to-head side (middle) and front (RIGHT) view at 9 ns, of MD simulation; row #3: smooth-rough, head-to-head front (LEFT) and side (middle) view at 8 ns, smooth-rough, head-to-tail (RIGHT) at 10 ns, of MD simulation; row #4: smooth-rough, head-to-head side (LEFT), stick model, front (middle) and CPK model, front (RIGHT) view at 4 ns of

MD simulation; Bottom, row #5: smooth-smooth, head-to-tail 7 β -OOH-Chol front (LEFT), Chol front (middle) and side (RIGHT) view at 4 ns of MD simulation.

Table S1. Number of water molecules H-bonded to the polar groups of a sterol molecule in the dimer

Sterol/Polar group	Chol	O7a	O7b	OO7a	OO7b
OH-C3	2.46 \pm 0.70	2.46 \pm 0.70	2.41 \pm 0.68	2.36 \pm 0.68	2.37 \pm 0.70
O-C3	1.56 \pm 0.60	1.54 \pm 0.60	1.50 \pm 0.59	1.46 \pm 0.59	1.48 \pm 0.59
H-C3	0.90 \pm 0.33	0.91 \pm 0.30	0.91 \pm 0.30	0.90 \pm 0.32	0.89 \pm 0.32
OH-C7/ OOH-C7		2.05 \pm 0.78	2.10 \pm 0.73	2.84 \pm 1.01	2.71 \pm 1.07
O-C7		1.35 \pm 0.61	1.31 \pm 0.60	1.06 \pm 0.71	0.95 \pm 0.67
H-C7		0.70 \pm 0.46	0.78 \pm 0.42	0.86 \pm 0.35	0.85 \pm 0.37
O _{ET} -C7				0.92 \pm 0.63	0.92 \pm 0.66
Total	2.46 \pm 0.70	4.51 \pm 1.0	4.51 \pm 1.0	5.20 \pm 1.2	5.08 \pm 1.3

Average numbers of H-bonded water molecules to OH and OOH groups attached to the C3 and C7 atoms of a sterol molecule in Chol-Chol and Chol-oxChol dimers and separately to the hydroxy and ether oxygen (O-C3, O-C7, O_{ET}-C7) and hydrogen (H-C3, H-C7) atoms of Chol; 7 α -OH-Chol (O7a); 7 β -OH-Chol (O7b); 7 α -OOH-Chol (OO7a); 7 β -OOH-Chol (OO7b) in water. The total number of H-bonded water molecules to a sterol molecule in the dimer are given in the bottom row.

Supplementary Film 1. The process of Chol-Chol dimer formation in water and the subsequent behaviour of the Chol molecules in the dimer during 10 ns of MD simulation. One of the Chol molecules is fixed in space so it is neither translating nor rotating but the motions of its atoms are not restricted. The water molecules are not shown in the film for clarity. To each Chol molecule a local orthogonal coordinate frame is assigned and its axes are drawn in *red*, *green* and *blue*. The relative orientation of the two molecules is defined by three angles formed between the corresponding axes of the frames. The distance between the molecules is measured as C6-C6, C10-C10 and C13-C13 distances of the corresponding C6, C10 and C13 atoms of both molecules (see text). Below the film, there are graphs showing time courses of the three distances and the three angles. The colours of the angles correspond to the colours of the frame axes. The colours of the C6-C6, C10-C10 and C13-C13 distances are *red*, *green* and *blue*, respectively. The vertical *black* line moving along the time axis connects current configuration of the molecules in the film with the numerical values of distances and angles. When blue and green angles are $\sim 180^\circ$, the dimer configuration is smooth-smooth, when $\sim 0^\circ$, the dimer configuration is smooth-rough.

Supplementary Film 2. Dehydration of the contacting surfaces of two Chol molecules on dimer formation and the formation of a water cross-layer, *CLI*. The film shows how water molecules from the first hydration shell, *LI*, of each Chol molecule redistribute when the molecules approach each other in water. Water molecules other than those from *LI* and *CLI* are not shown in the film for clarity. Initially, the *LI* water surrounds the whole Chol molecule. When the molecules get closer, the shells of both molecules start sharing water molecules and forming *CLI*. The *CLI* gradually increases and concomitantly water molecules from *LI* move away from the contact surface. Eventually, the contact surfaces of both molecules get totally dehydrated and *CLI* stops growing. Every 50 ps the film is suspended and the whole system is rotated to better show distribution of water molecules around the dimer and the intermolecular space vacated by water. The Chol and *LI* water molecules are in line representation and *CLI* water molecules are in thick stick representation. All atoms are represented in standard colours but the carbon atoms of one Chol molecule are *yellow* and of the other are *green*.

References

1. Moss, G. P. (1989) Joint Commission on Biochemical Nomenclature. The nomenclature of steroids. *Eur J Biochem* **186**, 429-458
2. Szczelina, R., and Murzyn, K. (2014) DMG-alpha-A Computational Geometry Library for Multimolecular Systems. *Journal of Chemical Information and Modeling* **54**, 3112-3123
3. Abraham, M. J., Murtola, T., Schulz, R., Pall, S., Smith, J. C., Hess, B., and Lindahl, E. (2015) GROMACS: High performance molecular simulations through multi-level parallelism from laptops to supercomputer. *SoftwareX* **1-2**, 19-25
4. Branch, M. A., Coleman, T. F., and Li, Y. Y. (1999) A subspace, interior, and conjugate gradient method for large-scale bound-constrained minimization problems. *Siam J Sci Comput* **21**, 1-23